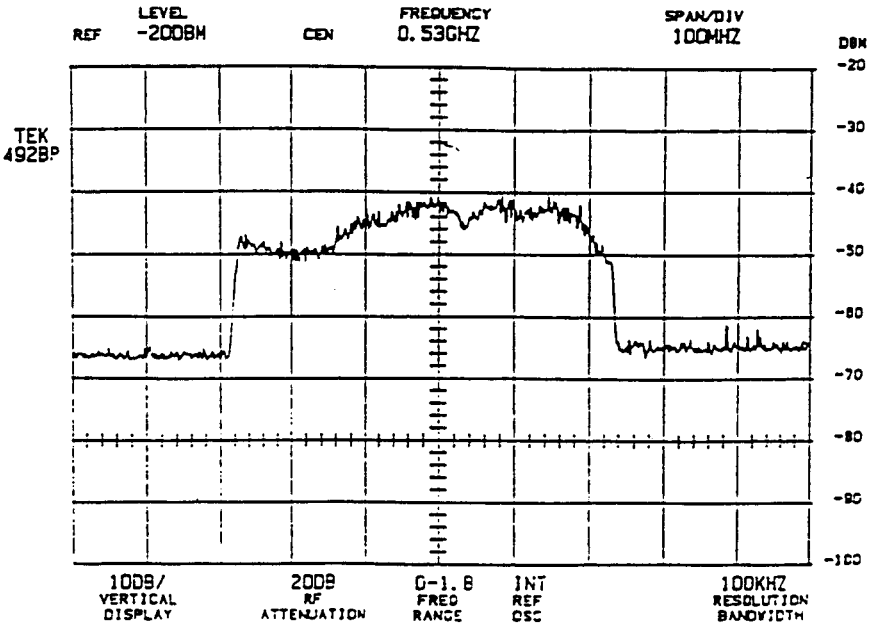

Figure 5 Spectrum of the IF signal measured

signal incident onto the antenna as for the receiver. Figure 3 shows the measurement setup with the two standard horns 3.0 m away from the antenna. The incident RF signal swept from 5.0 to 6.0 GHz with an output power of 8 dBm.

Figure 4 shows the spectrum of the radiating signal from the transmitter. The measured central frequency is 6.002 GHz, only 0.03% deviation from the designed transmitting frequency of 6.0 GHz. Figure 5 gives the IF output of the mixer, recorded by a Tek spectrum analyzer. The IF signal ranges from 250 to 750 MHz, and has a bandwidth of 500 MHz. It corresponds to the RF incident signal sweeping from 5.25 to 5.75 GHz. The IF signal has a maximum response around 500 MHz that corresponds to a receiving resonant frequency of 5.0 GHz, the same as the designed value.

IV. CONCLUSIONS

A design using one single local oscillator for transmitting and receiving duplex circuitry was presented. A "proof-of-concept" prototype was successfully developed and tested. Although the prototype using a rectangular patch antenna to achieve the LO coupling is shown, other application-specific designs with other types of antennas can be carried out with a similar principle. Such a design is compact, and has potential applications both in short-range communication and millimeter-wave systems.

REFERENCES

1. J. Lin and T. Itoh, Active integrated antenna, IEEE Trans Microwave Theory Tech 42 (1994), 2186–2194.
2. J.A. Navarro and K. Chang, Integrated active antennas and spatial power combining, Wiley, New York, 1996.
3. C.M. Montiel, L. Fan, and K. Chang, A novel active antenna with self-mixing and wideband varactor-tuning capabilities for communication and vehicle identification applications, IEEE Trans Microwave Theory Tech 44 (1996).
4. K. Cha, S. Kawasaki, and T. Itoh, Transponder using self-oscillating mixer and active antenna, Dig IEEE Int Microwave Symp, San Diego, CA, May 1994, pp. 425–428.
5. M.J. Cryan, P.S. Hall, S.H. Tsang, and J. Sha, Integrated active antenna with full duplex operation, IEEE Trans Microwave Theory Tech 45 (1997), 1742–1748.
6. I.J. Bahl and P. Bhartia, Microstrip antenna, Artech House, Dedham, MA, 1980.

Ti:SAPPHIRE LASER-PUMPED SELF-*Q*-SWITCHED Cr, Nd:YAG LASER WITH SINGLE-LONGITUDINAL-MODE OUTPUT

Jun Dong,[1] Peizhen Deng,[1] Yinghua Zhang,[1] Yupu Liu,[1] Jun Xu,[1] and Wei Chen[1]
[1] Shanghai Institute of Optics and Fine Mechanics
Chinese Academy of Sciences
Shanghai 201800, P.R. China

Received 25 January 2000

ABSTRACT: *We report the operation of a CW Ti:sapphire laser-pumped monolithic self-Q-switched Cr, Nd:YAG laser in which the codoped chromium ions act as saturable absorbers for Nd^{3+} laser emission at 1064 nm. The laser slope efficiency is as high as 22%, the pulse width is as short as 12 ns, and the laser modes are very stable. The use of a laser host crystal codoped with a saturable absorber and a laser gain medium can lead to the development of monolithic self-Q-switched solid-state lasers.* © 2000 John Wiley & Sons, Inc. Microwave Opt Technol Lett 26: 124–127, 2000.

Key words: *Cr, Nd:YAG crystal; self-Q-switched laser, Ti:sapphire laser*

1. INTRODUCTION

In recent years, Cr^{4+}-doped crystals have attracted a great deal of attention as passive *Q*-switches [1–4]. These Cr^{4+}-doped crystals include Cr^{4+}:YAG [1, 2], Cr^{4+}:GSGG [3], Cr^{4+}:YSO [4], etc. They have a large absorption cross section and low saturable intensity at the laser wavelength. In com-

parison with previously used saturable absorbers such as dyes [5] and LiF:F_2^- color center crystals [6], Cr^{4+}-doped crystals are more photochemically and thermally stable and have a higher damage threshold. They can be used as *Q*-switches for both pulsed lasers [1, 3, 4] and continuously pumped lasers [2]. Moreover, Cr^{4+}:YAG can be codoped with an amplifying medium in a monolithic structure to form a self-*Q*-switched laser [2]. As a result of the above-mentioned advantages, Cr^{4+}-doped crystals have become the most promising saturable absorbers for passively *Q*-switched lasers of stability, low cost, reliability, long life, compactness, and simplicity. So we have studied the laser performance of Cr, Nd:YAG crystals with Ti:sapphire as the pump source.

2. EXPERIMENTAL SETUP

The Cr, Nd:YAG crystal used in the experiment was grown by using the standard Czochralski (CZ) method. Cr^{4+} is to be substituted into the tetrahedral Al^{3+} site; therefore, a charge compensator is required, and a divalent calcium ion was added as the charge compensator. Samples for spectroscopic measurements were cut out of boules, and the surfaces perpendicular to the ⟨111⟩ growth axis were measured using a Lambda Perkin-Elmer 9 UV/VIS/NIR spectrometer at room temperature. The schematic of a CW Ti:sapphire laser-pumped Cr, Nd:YAG self-*Q*-switched laser cavity is shown in Figure 1. A Cr, Nd:YAG crystal was polished to a planar–planar geometry. The rear surface of the Cr, Nd:YAG crystal is coated for high transmission at 808 nm and total reflection at 1064 nm. The front surface is coated for total reflection at 808 nm and 95% reflection at 1064 nm as the output coupler. The misalignment of the axes of the two mirrors is measured to be less than 0.3°. The laser operation was performed at 278 K by using constant-temperature water-cooled circulation with a copper surface. The *Q*-switched pulses were recorded using a fast Si *p-i-n* detector with a 1.5 ns rise time and a Tektronix TDS 380 digitizing oscilloscope with a 400 MHz sampling rate in the single-shot mode. The output power was measured using a laser power meter. The Ti:sapphire laser output, after beam shaping with a focal lens, is focused onto a spot with a diameter of 50 μm. The Ti:sapphire laser is operated in the CW mode, and after the focal lens, the loss is approximately 8%.

3. RESULTS AND DISCUSSIONS

After correcting the surface reflection losses, the room-temperature absorption spectrum of the Cr, Nd:YAG crystal is displayed in Figure 2. The absorption feature in the visible region is similar to that of chromium-doped YAG [7]. The absorption bands peaking at 0.53, 0.59, 0.75, 0.81, and 0.88 μm are attributed to Nd^{3+} ions. The broad absorption bands centered at 0.43 and 0.59 μm are attributed to the $^4A_2 \rightarrow {}^4T_1$ and $^4A_2 \rightarrow {}^4T_2$ transitions of Cr^{3+}. The band from 900 to 1200 nm is believed to be caused by Cr^{4+} ions [8]. The absorption coefficient is 2.6 cm^{-1} at a pumping wavelength of

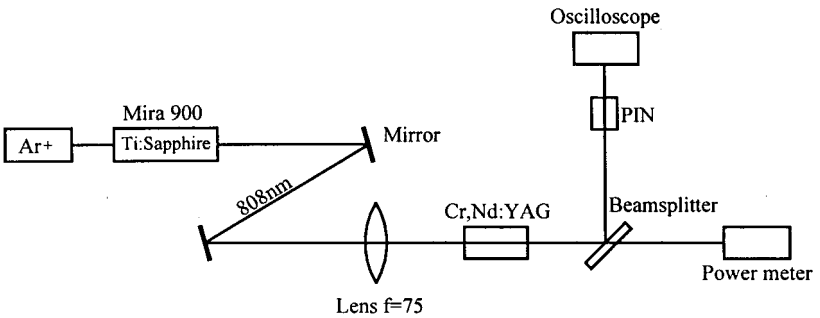

Figure 1 Schematic of Ti:sapphire-pumped self-*Q*-switched Cr, Nd:YAG laser experimental setup

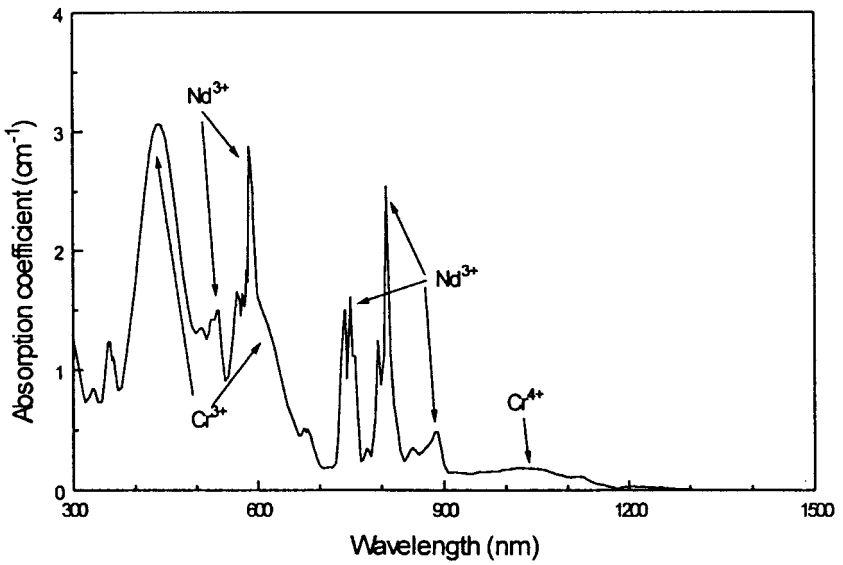

Figure 2 Room-temperature absorption spectrum of Cr, Nd:YAG crystal

808 nm, and is 0.15 cm^{-1} at 1064 nm. With Cr, Nd:YAG crystal as the active medium, the laser Q switches, and the output mode is single-longitudinal-mode stable. Figure 3 shows a typical Q-switched pulse shape with an output energy of 2.7 μJ and an FWHM duration of 12 ns. The peak power is estimated to be 225 W.

Figure 4 shows the output power versus input pump power of a self-Q-switched Cr, Nd:YAG laser. The performance of the self-Q-switched laser was corrected for Fresnel losses. From Figure 4, we see that the threshold pumping power is approximately 90 mW, and the slope efficiency is as high as 22%. Although Q-switched lasers generally have larger intensity fluctuations, we have found that the Q-switched pulse amplitude is extremely stable. The pulse-to-pulse intensity fluctuation is less than the instrument resolution of 0.25%, which merely reflects the small fluctuation of the baseline of the oscilloscope traces. This unprecedented stability is attributed to the stable pump beam of the Ti:sapphire laser and the cavity that is free from mechanical vibrations. No deterioration in intensity stability was detected over a continuous 3 h testing period.

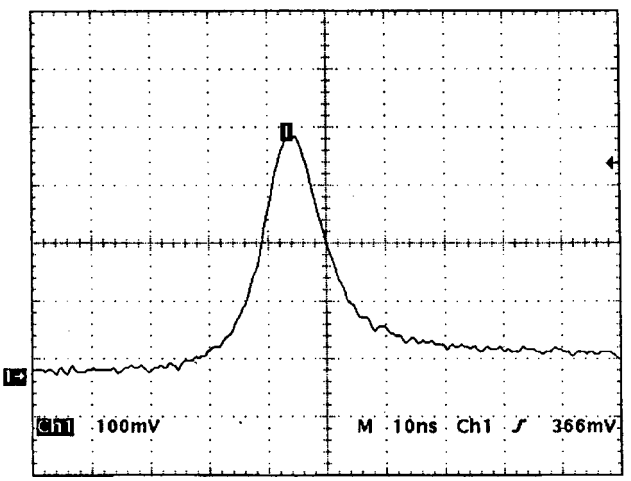

Figure 3 Oscilloscope trace of the self-Q-switched Cr, Nd:YAG laser with an FWHM duration of 12 ns

During the Q-switched laser experiment, the pulse width keeps constant with the variation of the input pumping power, and the pulse repetition rate varies with the variation of the input pumping power; with an increase of the pumping power, the pulse repetition rate increases. The pulse width keeping constant may be due to the low pumping power; the pumping power density is not high enough to change the pulse width. The other reason for the pulse width keeping constant with an increase of the pumping power may be because the pulse width depends on the initiation transmission of the saturable absorber Cr^{4+} in a Cr, Nd:YAG crystal. We also found that the Q-switched laser pulse is linearly polarized along either of the mutually orthogonal axes with an extinction ratio of 200:1. By rotating the polarization of the pump beam, the laser polarization between the two axes is switched. The crystal used in this experiment exhibits neither birefringence nor anisotropic transmission for low levels of light intensity. The polarized laser output of Cr, Nd:YAG is probably caused by the anisotropy in the saturation power of the absorber.

4. CONCLUSIONS

A self-Q-switched Cr, Nd:YAG laser operated with a Ti:sapphire laser as the pumping source. We have demonstrated that the output Q-switched traces are very single-longitudinal-mode stable, the threshold pumping power is as low as 90 mW, and the pulse duration is as short as 12 ns. And the pulse width keeps constant and pulse repetition rate varies with the variation of the pumping power. This can lead to development of monolithic self-Q-switched solid-state lasers.

REFERENCES

1. P. Yankov, Cr^{4+}:YAG Q-switching of Nd:host laser oscillators, J Phys D 27 (1994), 1118–1120.
2. S. Zhou, K.K. Lee, and Y.C. Chen, Monolithic self-Q-switched Cr, Nd:YAG laser, Opt Lett 18 (1993), 511–512.
3. W. Chen, K. Spariosu, and R. Stultz, Cr^{4+}:GSGG saturable absorber Q-switched for the ruby laser, Opt Commun 104 (1993), 71–74.
4. Y.K. Kou, M.F. Huang, and M. Birnbaum, Tunable Cr^{4+}:YSO Q-switched Cr:LiCAF laser, IEEE J Quantum Electron 31 (1995), 657–663.

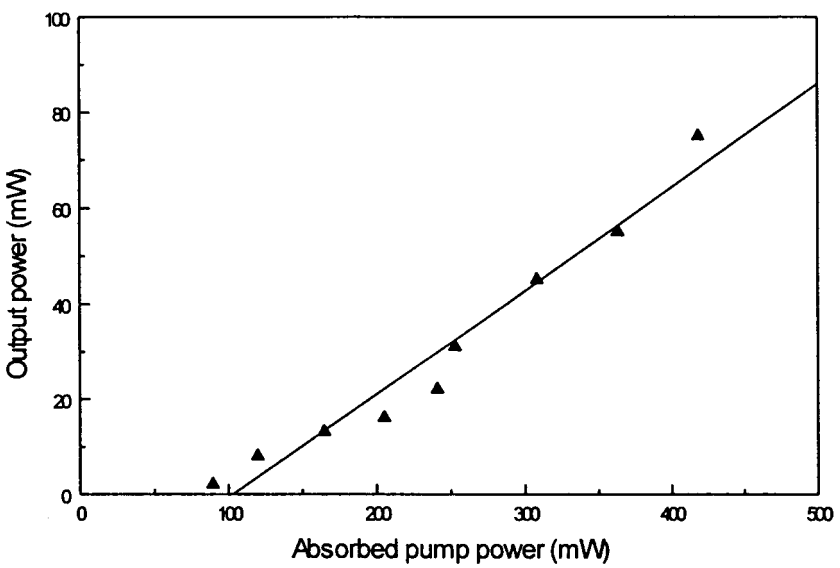

Figure 4 Relation between the output power and the input pumping power

5. W. Kochner, Solid state laser engineering, Springer-Verlag, Berlin, Germany, 1992, 3rd ed., chap. 8.
6. J.A. Morris and C.R. Pollock, Passive Q-switching of a diode-pumped Nd:YAG laser with a saturable absorber, Opt Lett 15 (1990), 440–442.
7. N.B. Angert, N.I. Borodin, V.M. Garmash et al., Lasing due to impurity color centers in yttrium aluminum garnet crystals at wavelengths in the range 1.35–1.45 μm, Sov J Quantum Electron 18 (1988), 73–74.
8. V. Petricevic, S.K. Gayen, and R.R. Alfano, Laser action in chromium-activated forsterite for near-infrared excitation: Is Cr^{4+} the lasing ion?, Appl Phys Lett 53 (1988), 2590–2592.

SURFACE IMAGE GENERATION USING LOCAL SLOPE-BASED MAPPING ALGORITHM

Sarit Pal[1] and S. K. Kak[1]
[1] Fiber Optics and Optical Communication Laboratory
Department of Electronics Engineering
Institute of Technology
Banaras Hindu University
Varanasi 221005, India

Received 6 January 2000

ABSTRACT: *This paper introduces a novel technique to provide the microtopographical details of a machined surface using a fiber-optic probe. Unlike the previous methods, the present approach involves pixel-to-pixel scanning for slope measurement, which in turn generates the three-dimensional profile of the probed surface using the relevant mapping algorithm. Minute details of the surface roughness characteristics, including slope and height at different positions, can be visualized from the reconstructed surface image.* © 2000 John Wiley & Sons, Inc. Microwave Opt Technol Lett 26: 127–132, 2000.

Key words: *fiber-optic sensors; image sensors; optical profilometer; signal processing; precision surface metrology; surface roughness; mapping algorithm*

1. INTRODUCTION

The certification of a flat surface has been a long-standing problem with various forms and degrees of solutions. In the modern computer-integrated industry, statistical process control plays an important role. The increasingly higher standards of on-line quality tests necessitate new, fast, flexible sensors which should, as far as possible, be noninteracting, to record individual quality characteristics directly in the production environment. Surface topology plays a vital role in design, development, processing, and quality control in manufacturing process. Absolute calibration of an optical flatness was defined by Fritz [1]. The problem of characterizing the surface topography of optically smooth surfaces has been approached from several directions over the last decade. Optoelectronic sensors with a signal processing algorithm provide a good basis for the implementation of quality control in the process environment. Optical techniques to characterize the surface finish are increasingly used in industrial applications as these techniques have several advantages over classical mechanical methods. Due to the advancement of the fiber-optic technique, various types of fiber-optic sensors were developed to study surface topology, including the different techniques for on-line and in-line inspection and production measurement in industries [2–14]. Among the various optical methods used to study surface topology, laser light scattering is one of the most promising approaches for on-line/in-process precision surface metrology. A reflection- and scattering-based new technique to measure the surface roughness in terms of local slope was proposed in our previous work [15]. The method for free-form surface reconstruction for machine vision was proposed by Bradley and Vickers [13], whereas vision-based coordinate measurement and image formation of a surface have been described by El-Hakim and Pizzi [16].

In this paper, the focus is on the methodology and the relevant algorithm developed for surface reconstruction. A high-speed and automatic artificial vision technique for accurate measurement of the local slope as the surface roughness parameter, and also to generate a surface model based thereupon, is presented. For this purpose, a sensor is developed to satisfy the requirement that it should be

- able to make measurements on a surface in a noncontact and nondestructive manner with high accuracy
- able to provide simultaneously the information regarding the three-dimensional coordinate values of a point on a surface and the inclination of the surface at that point
- able to measure various grades of rough surfaces continuously with high speed
- compact and flexible so that the sensor can be incorporated into computer-aided manufacturing (CAM).

This proposed system consists of an optical-fiber-based surface scanning system for slope measurement along with the surface modeling software. At first, the theory is developed to measure the local slope of the probed surface, and afterwards, the mapping algorithm is formulated, which has generated the three-dimensional representation properly.

2. THEORY AND PRINCIPLES OF SURFACE RECONSTRUCTION

The three-dimensional representation of the surface can be generated from the information regarding the parameters such as tilt and orientation, height, etc., of the microelements (elements of areas—pixels) forming the entire surface, with respect to a standard perfectly smooth plane. The present paper describes the surface reconstruction technique using the mapping algorithm, based on the tilt and orientation angle of the microelements of the surface. The mapping algorithm relates the position of the pixel to its tilt and orientation, and hence to the coordinates of the corners of the pixels to construct the representation of the surface. The minute details of the surface roughness can be generated and displayed on a computer screen by feeding the angle of tilt and orientation through the software using this mapping algorithm. To analyze theoretically, the following assumptions have been made.

1. The surface can be represented by a continual combination of small elementary areas (microelements—pixels) with different tilts and orientations.